Magnetic Coupling of Porphyrin Molecules Through Graphene

*Christian F. Hermanns, Kartick Tarafder, Matthias Bernien, Alex Krüger, Yin-Ming Chang, Peter M. Oppeneer, and Wolfgang Kuch**

Graphene, a material with unique properties,[1] is expected to complement todays Si-based information technology with new and more efficient functions.[2–4] It exhibits desirable properties for spin electronic applications such as high charge carrier mobility, low intrinsic spin-orbit interaction, as well as low hyperfine interaction.[5–6] In particular, magnetic molecules in contact with graphene constitute a tantalizing approach towards organic spin electronics because of the reduced conductivity mismatch at the interface. In such a system a bit is represented by a single molecular magnetic moment, which must be stabilized against thermal fluctuations.[7] Here, we show in a combined experimental and theoretical study that the moments of paramagnetic Co-octaethylporphyrin (CoOEP) molecules on graphene can be aligned by a remarkable anti-ferromagnetic coupling to a Ni substrate underneath the graphene. This coupling is mediated via the π electronic system of graphene, while no covalent bonds between the molecule and the substrate are established, and the molecules sit at a distance of ≈3.3 Å above the graphene plane. The laterally extended π electron system of graphene exhibits metal-like electronic properties along the plane, and molecule-like properties perpendicular to the plane, which makes graphene highly relevant for the design of hybrid metal-organic spintronic materials. Several studies have focused on the spin-split electronic states of graphene or the injection of spin-polarized currents from metallic ferromagnetic electrodes.[8–10] Electronic spin transport and spin precession have been observed in graphene over micrometer distances even at room temperature.[11,12] Molecules adsorb on graphene mainly by Van der Waals interaction, thereby the molecular properties of the adsorbate, like its reactivity, are preserved. This opens the door to an optimization of the undisturbed molecular design of an adsorbate independently of its interaction with the substrate.

We use X-ray magnetic circular dichroism (XMCD) in the absorption of soft X rays as an element-selective probe of the magnetization of CoOEP molecules in the submonolayer regime on a graphene-passivated Ni film,[13] supported by a W(110) single crystal surface. In the upper and lower panel of Figure 1a, we show Co $L_{2,3}$ X-ray absorption (XA) spectra and XMCD spectra of 0.7 molecular monolayers (ML) of CoOEP on top of graphene/Ni, respectively, measured in zero field at remanence of the ferromagnetic Ni film. The astonishing presence of a finite Co XMCD signal proves on the one hand a net 3*d* magnetic moment localized on the Co ions and on the other hand an unexpected magnetic coupling between the magnetization of the Ni layer and these Co moments, stabilizing them against thermal fluctuations. The XA spectrum as well as the XMCD spectra exhibit a particular finestructure at the Co L_3 edge, which, by comparison to CoPc bulk measurements,[14] is consistent with a d^7 low-spin state of Co. The XMCD difference curves in Figure 1a show a positive excursion at the Co L_3 edge between about 777 and 781 eV photon energy, which is about a factor 4.1 larger at 30 K compared to 130 K, and only a small negative signal at the Co L_2 edge at around 793.5 eV. The sign of this XMCD signal is opposite to that of the ferromagnetic Ni layer underneath the graphene, displayed in the inset of the upper panel of Figure 1a. This proves an anti-ferromagnetic coupling between the magnetic moments of the Co centers and the Ni magnetization.

By employing the XMCD spin sum rule on the Co XMCD spectrum measured at 30 K,[15] an effective spin magnetic moment of (0.87 ± 0.05) μ_B is obtained. As the Co magnetic moments are subject to thermal fluctuations at finite temperatures, this value presents a lower limit. The effective spin magnetic moment fits to a low-spin $S = 1/2$ configuration of the Co ions. The coupling energy E_{ex} between the Co spins and the Ni substrate can be estimated from the Co magnetization relative to the one of Ni as a function of temperature, assuming that all molecules interact in the same manner with the surface. In Figure 1b the Co and Ni L_3 XMCD signals, normalized to their extrapolated saturation values, are plotted vs. temperature. The temperature progression of the Co and Ni magnetizations clearly differs. Experimental data are shown together with a theoretically modeled temperature dependence of the respective magnetization. A Brillouin function $B_J(\alpha)$ with $\alpha = E_{ex}/(k_B T)$, temperature T, and Boltzmann constant k_B is used to represent the relative Co magnetization, incorporating the coupling to the magnetic substrate as an effective magnetic field and neglecting magnetic anisotropy:[16]

$$M_r^{Co}(T) = M_r^{Ni}(T)\, B_J(\alpha) \quad (1)$$

As an exchange field acts directly on the spin, $J = 1/2$ and a temperature-independent coupling energy E_{ex} is assumed. The fit yields E_{ex} = (1.8 ± 0.5) meV for the data acquired at temperatures between 30 and 130 K. Thereby the Ni magnetization is modeled by a $(1 - T/T_C)^\beta$ law, with a Curie temperature of T_C = 630 K and a critical exponent $\beta = 0.365$.[17] The strength of

C. F. Hermanns, Dr. M. Bernien, A. Krüger, Dr. Y.-M. Chang, Prof. W. Kuch
Institut für Experimentalphysik
Freie Universität Berlin
Arnimallee 14, 14195 Berlin, Germany
E-mail: kuch@physik.fu-berlin.de
Dr. K. Tarafder, Prof. P. M. Oppeneer
Department of Physics and Astronomy
Uppsala University
P. O. Box 516, 75120 Uppsala, Sweden

DOI: 10.1002/adma.201205275

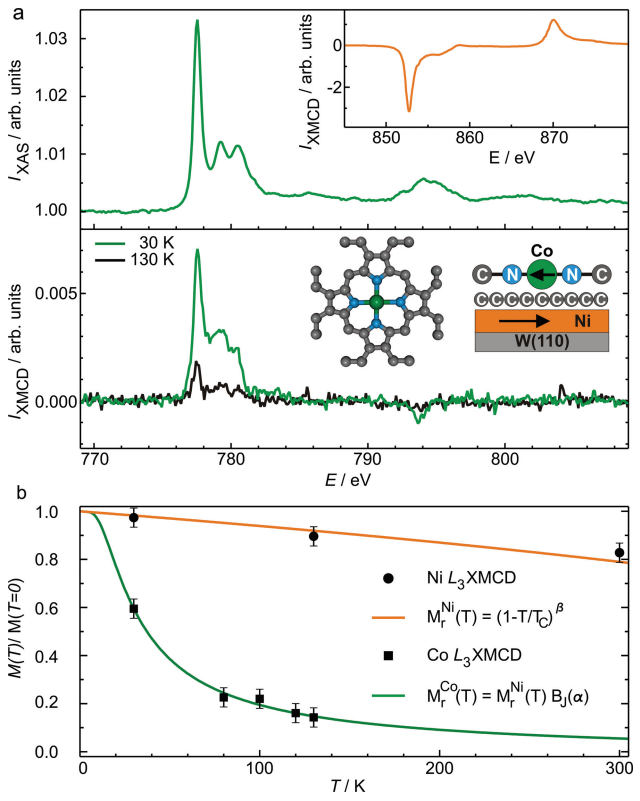

Figure 1. a) Co $L_{2,3}$ XAS (upper panel) and XMCD (lower panel) spectra of 0.7 ML CoOEP on graphene/Ni/W(110) measured at 70° grazing incidence at 30 K (green lines) and 130 K (black line). Insets: (upper panel) XMCD spectrum at the Ni $L_{2,3}$ edges (orange line) at 130 K showing opposite sign at the L_3 and the L_2 edges compared to the Co XMCD spectrum; (lower panel) schematic top view of CoOEP molecule and side view of the sample, where the green, blue, and grey balls represent cobalt, nitrogen, and carbon atoms, respectively, and hydrogen atoms are omitted. b) Temperature dependence of Co XMCD (squares: experimental data; green full line: fit of Brillouin-type model) and Ni XMCD (circles: experimental data; orange full line: $(1 - T/T_C)^{\beta}$ with T_C = 630 K and β = 0.365) for 0.7 ML CoOEP on graphene/Ni/W(110).

the magnetic coupling across the graphene layer as opposed to metalloporphyrins adsorbed directly on reactive ferromagnetic substrates is comparatively small.[16,18]

To shed light on the unexpected exchange coupling of paramagnetic metalorganic molecules mediated through graphene, we have performed ab initio calculations employing the DFT+U approach (see Methods section for details). In recent studies of graphene on Ni(111) six possible arrangements of the graphene atoms on a Ni(111) surface have been discussed, the most prominent ones are denoted as the bridge-top, top-fcc, top-hcp, and fcc-hcp configurations.[19–23] For these four configurations, the three more symmetric ones and the bridge-top configuration that had been favored by DFT calculations,[20,24] we have performed geometrical optimizations and ab initio calculations of the molecule-substrate exchange interaction. Our calculations were performed both with and without Van der Waals (VdW) correction terms.[25] The bridge-top configuration has the lowest computed total energy;[20] consistently, we find that this adsorption geometry gives agreement between measured and calculated results. Also for hcp-fcc adsorption geometry an antiparallel alignment of Ni and Co spins is computed, however, this arrangement leads to a higher total energy. Therefore, only the results computed for the bridge-top geometry are analyzed further in the following. For completeness' sake we present the computed electronic and magnetic properties of the system also for the three other graphene-Ni adsorption geometries in the Supporting Information (see Figure S6).

The porphyrin molecule is computed to adsorb in planar geometry on graphene, with a slight bending of the macrocyclic rings towards the substrate. This is consistent with results of angle-dependent XA measurements at the carbon and nitrogen K edge (see Figure S3 and S4 in the Supporting Information). The VdW correction has a small influence on the equilibrium distances between the Ni top layer and graphene, and between graphene and the central metal ion. The Ni-graphene distance is 2.08 Å, whereas the graphene-metal ion distance is 3.68 Å (without VdW) and 3.51 Å (with VdW) for the bridge-top configuration. The VdW corrections thus reduce the molecule-graphene distance slightly (≈5%), while interatomic distances in the porphyrin molecule are not affected. The computed optimal planar position of the Co ion is near the center of the hexagon formed by graphene C atoms.

Our ab initio DFT+U calculations predict, in the equilibrium adsorption position, a low spin S = 1/2 state of the Co ion and an antiparallel alignment of its magnetic moment with respect to the Ni magnetization, consistent with experiment. **Figure 2** shows an atom-projected and spin-resolved density-of-states-plot for the Co porphyrin/graphene/Ni system, which additionally reveals a small spin polarization on the N atoms, antiparallel to that of the Co ions. Unraveling further the origin of the coupling behavior, we consider the d-orbital occupations of the central ion and the resulting magnetization density. The seven 3d electrons of the Co ion are distributed over the three filled $d_{yz,xz}$ and d_{xy} orbitals and the half-filled $d_{3z^2-r^2}$ orbital, which determines the magnetization density distribution on the Co ion (see Figure S8 in the Supporting Information for the DOS of the Co 3d orbitals). **Figure 3**a shows the ab initio computed magnetization densities (with VdW) of a Co porphyrin molecule on graphene supported on Ni. The negative magnetization density on the Co center, shown in light blue, has the expected $d_{3z^2-r^2}$-type shape. At first sight one might suppose that a direct exchange coupling of Co occurs through hybridization of the $d_{3z^2-r^2}$ and graphene p_z orbitals, however, a closer inspection showed that this is not the case. To shine light on the electronic wavefunction overlap in space we present in Figure 3b a charge density cross-section plot. This plot illustrates that the electronic interaction between the porphyrin molecules and graphene occurs due to little overlap of macrocyclic π and graphene p_z orbitals; the overlap of the short-ranged metal 3d and graphene p orbitals is negligible, as can be seen from the dip in the charge density at the Co site. This is also evident from isotropic XAS measurements at the cobalt L_3 edge of CoOEP molecules in a polycrystalline bulk sample, on graphene/Ni/W(110), and on bare Ni films (see Figure S5 in the Supporting Information). Considering the possible exchange paths from the Ni top layer to the metal center, we observe the following: A small negative spin density on graphene (–0.001μ_B), shown in light blue in Figure 3a, which is antiparallel to the dominant one on Ni, is induced in the graphene upper π-bond lobe of the C–C bridge (above a

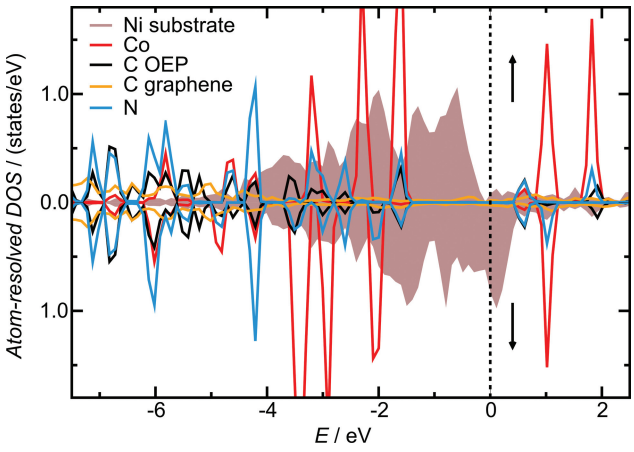

Figure 2. Atom-projected and spin-resolved density of states (DOS) of a Co porphyrin molecule on graphene/Ni(111) obtained from DFT+*U* calculations. The spin polarization on the Co ions is antiparallel to that of the Ni substrate seen from the opposite shifts of the spin majority DOS. Positive atomic DOS corresponds to spin up, negative atomic DOS to spin down.

surface Ni atom). The lower π-bond lobe has acquired a positive magnetization density, which interconnects to a network. This results from hybridization with spin-minority Ni *sp* states (seen as extended light blue framework) with graphene p_z orbitals. A weak antiparallel coupling between graphene π and porphyrin π orbitals induces a small positive spin density, residing mainly on the pyrrolic nitrogen atoms (+0.015μ_B), being thus parallel to the 3d spin density on Ni. This small parallel spin-density on the nitrogen atoms can be recognized in Figure 3a by the yellow contours. The final chain in the exchange path is the magnetic coupling between the nitrogen atoms and the central Co ion. The N *p* orbitals hybridize weakly with the Co $d_{3z^2-r^2}$ orbital favoring an antiparallel spin polarization on N and Co. Consequently, our ab initio calculations unveil an indirect-direct double exchange interaction between the top-layer Ni spin and the central Co ion's spin: The graphene π-bonded sheet mediates a weak superexchange between the spin polarization of Ni and the pyrrolic nitrogens; the spin densities of the latter couple through direct exchange to the spins on the central ion of the molecule.

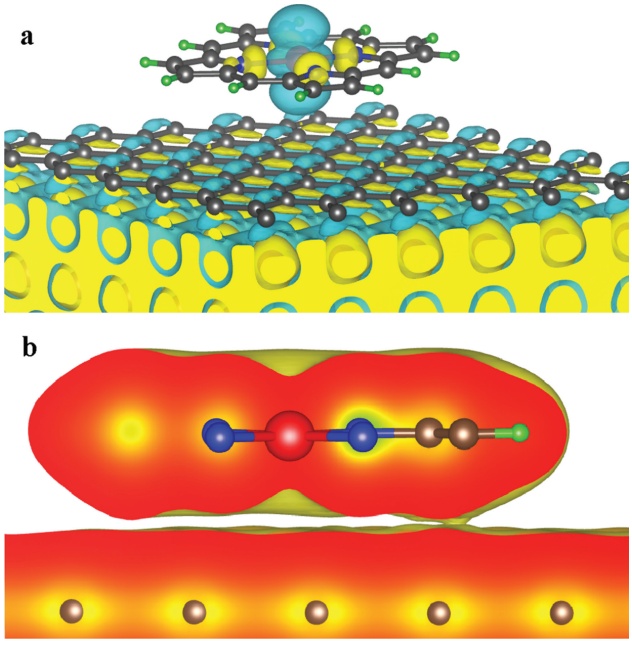

Figure 3. a) Calculated magnetization density of a Co porphine adsorbed on graphene/Ni. The bright yellow hypersurfaces show contours of positive magnetization densities, the light blue hypersurface shows contours of negative magnetization density. Note the small positive magnetization densities present on the nitrogen atoms. b) Charge density cross-sectional plot of a Co porphine adsorbed on graphene/Ni. The cross-section reveals a negligible overlap with the graphene charge density at the Co site. (Used isosurface values: 30 eV Å^{-3}).

Magnetism of a Cr-containing molecule on a graphene sheet has been predicted, however, without a stabilizing mechanism for the spin, rendering the system to be paramagnetic.[7] Also, for graphene in contact with pure metal layers magnetism was predicted,[26] but an experimental confirmation is missing. Here, the graphene layer, on the one hand, decouples the molecules from the substrate and passivates the Ni surface.[13] Similar organic molecules as the here-studied ones, Fe phthalocyanines, have been also found decoupled electronically from the substrate on a graphene-covered metal surface, where they maintained their molecular electronic properties.[27] This virtue of a weak electronic interaction permits to achieve design of molecular functionalities of an adsorbate undisturbed by its interaction with the substrate. On the other hand, the graphene layer also mediates a magnetic interaction between the molecules and the substrate, an essential ingredient for the use of paramagnetic molecules as building blocks of a molecular spin electronics. Such molecules had moved into the center of interest after it was shown that the spin of adsorbed metalloporphyrin molecules and Tb phthalocyanine double-deckers can be stabilized against thermal fluctuations by magnetic coupling to a ferromagnetic substrate at elevated temperatures.[16,18,28,29] Density functional theory calculations revealed that the magnetic coupling of the porphyrin molecules is of superexchange type.[16,18,30] In these cases, however, the exchange coupling was established by covalent bonds between the molecules and surface atoms forming a hybrid metal-organic interface, while in the case of graphene no covalent bond is formed. Our result encourages the pursuit of spin-electronic devices such as spin qubits or spin field-effect transistors by assembling planar paramagnetic molecules wired by graphene ribbons on a surface. Electronic transport through the molecules or switching their magnetic properties, for example, could be accomplished by taking advantage of the empty sixth coordination place.

Experimental Section and Theoretical Details

The graphene layer has been prepared on a Ni film deposited on a W(110) single crystal surface under ultrahigh vacuum conditions (p = 2.0 × 10^{-10} mbar), following the recipe described in refs.[8,9] A W(110) single crystal substrate was cleaned by flash heating under 6 × 10^{-8} mbar oxygen to 1600 K for 15 min, followed by five flashes to 2300 K for 10 s each. The surface quality was checked by low-energy electron diffraction. (111)-oriented Ni films of around 5.1 nm thickness were prepared by electron-beam evaporation on the clean W(110) substrate held at room

temperature, followed by annealing at 570 K for 10 min. A continuous and ordered graphene overlayer is prepared via cracking of propene gas (C_3H_6) at a partial pressure of 10^{-6} mbar for 10 min at a substrate temperature of 650 K, followed by annealing to 750 K for 10 min.[9] Co(II)-2,3,7,8,12,13,17,18-octaethylporphyrin molecules were purchased from Sigma Aldrich, and evaporated by sublimating molecular powder from a crucible at around 485 K onto the sample held at room temperature. Thicknesses and coverages were estimated using quartz microbalances integrated in the evaporators, and from comparison of the signal-to-background ratio at the respective XA edges to literature data.[31]

XA measurements were performed using X rays of the helical undulator beamline UE56/2-PGM1 of BESSY II in Berlin, with a circular degree of polarization of about 85%. XA spectra were acquired in total electron yield mode recording the sample drain current as a function of photon energy, while monitoring the incoming beam intensities by the total electron yield of a freshly evaporated gold grid. Furthermore, the XA spectra were normalized to the corresponding spectra measured of the clean substrate and scaled to 1 in the pre-edge energy region. The photon energy resolution was set to 300 meV. Magnetic measurements were carried out in remanence of the Ni film with a thickness of around 26 monolayers (ML) and an easy magnetization axis in the film plane.[32] Typical photon flux densities at the sample of about 10^{12} s^{-1} cm^{-2} were used to prevent radiation damage, which can be excluded here from the comparison of spectra taken immediately after sample preparation and at later times. Calibration of the photon energy was carried out by means of XA measurements of Co films on a Cu(100) crystal setting the position of the Co L_3 edge to 778.5 eV. Identical Co $L_{2,3}$ XA and XMCD spectra, with respect to the line-shape and results of the sum rule analysis, were obtained during different beamtimes for the system under study.

Ab initio calculations were performed with the density-functional theory +U (DFT+U) approach, wherein the strong electron-electron Coulomb interactions that exist in the open 3d shell of the 3d ion are captured by the supplemented Hubbard and exchange constants U and J. In the present calculations U and J were taken to be 4 eV and 1 eV, respectively. These values were previously shown to provide the correct spin state for free and adsorbed metalloporphyrins.[33,34] In addition our calculations were performed both with and without Van der Waals correction terms.[25] We employed the VASP full-potential plane-wave code, in which pseudo-potentials together within the projector augmented wave method are used.[35,36] A kinetic energy cut-off of 400 eV was employed for the plane waves. For the DFT exchange-correlation functional the generalized gradient approximation was used, in PBE parameterization.[37] The metallic surface was modeled through three atomic Ni layers (adopting the fcc Ni lattice parameter). For simplicity and to focus on the magnetic interaction in the center of the molecule, the ethylene peripheral groups were replaced by hydrogen atoms. Full geometric optimizations of the metalloporphyrin molecules, the graphene and Ni surface layer were performed, including all interatomic distances until the forces were smaller than 0.01 eV $Å^{-1}$. Recent DFT+U calculations revealed that metalloporphyrins on metallic substrates may exhibit two distinct adsorption distances;[34] for metalloporphyrins on graphene we obtained only a single adsorption distance. For the bridge-top adsorption geometry of graphene on Ni(111), a geometric relaxation of the graphene/Ni system was first carried out for the top Ni layer, the graphene layer, and the Co porphine position. For the reciprocal space sampling we used $3 \times 3 \times 1$ Monkhorst–Pack k points.

Supporting Information

Supporting Information is available from the Wiley Online Library or from the author.

Acknowledgements

B. Zada and W. Mahler are acknowledged for their technical support, and N. Reineking and A. Bruch for help during the measurements. This work has been supported by the DFG through Sfb 658, the BMBF (05K10KE1), the Swedish-Indian Research Link Programme, the C. Tryggers Foundation, and the Swedish National Infrastructure for Computing (SNIC).

Received: December 21, 2012
Revised: March 11, 2013
Published online: May 21, 2013

[1] A. K. Geim, K. S. Novoselov, *Nat. Mater.* **2007**, *6*, 183.
[2] K. V. Emtsev, A. Bostwick, K. Horn, J. Jobst, G. L. Kellogg, L. Ley, J. L. McChesney, T. Ohta, S. A. Reshanov, J. Röhrl, E. Rotenberg, A. K. Schmid, D. Waldmann, H. B. Weber, T. Seyller *Nat. Mater.* **2009**, *8*, 203.
[3] L. Britnell, R. V. Gorbachev, R. Jalil, B. D. Belle, F. Schedin, A. Mishchenko, T. Georgiou, M. I. Katsnelson, L. Eaves, S. V. Morozov, N. M. R. Peres, J. Leist, A. K. Geim, K. S. Novoselov, L. A. Ponomarenko, *Science* **2012**, *335*, 947.
[4] H. Yang, J. Heo , S. Park, H. J. Song, D. H. Seo, K.-E. Byun, P. Kim, I. Yoo, H.-J. Chung, K. Kim , *Science* **2012**, *336*, 1140.
[5] B. Trauzettel, D. V. Bulaev, D. Loss, G. Burkard, *Nat. Phys.* **2007**, *3*, 192.
[6] D. Huertas-Hernando, F. Guinea, A. Brataas, *Phys. Rev. B* **2006**, *74*, 155426.
[7] S. M. Avdoshenko, I. N. Ioffe, G. Cuniberti, L. Dunsch, A. A. Popov, *ACS Nano* **2011**, *5*, 9939.
[8] A. Varykhalov, J. Sánchez-Barriga, A. M. Shikin, C. Biswas, E. Vescovo, A. Rybkin, D. Marchenko, O. Rader, *Phys. Rev. Lett.* **2008**, *101*, 157601.
[9] Yu. S. Dedkov, M. Fonin, U. Rüdiger, C. Laubschat, *Phys. Rev. Lett.* **2008**, *100*, 107602.
[10] W. Han, K. Pi, K. M. McCreary, Y. Li, J. J. I. Wong, A. G. Swartz, R. K. Kawakami, *Phys. Rev. Lett.* **2010**, *105*, 167202.
[11] N. Tombros, C. Jozsa, M. Popinciuc, H. T. Jonkman, B. J. van Wees, *Nature* **2007**, *448*, 571.
[12] B. Dlubak, M.-B. Martin, C. Deranlot, B. Servet, S. Xavier, R. Mattana, M. Sprinkle, C. Berger, W. A. De Heer, F. Petroff, A. Anane, P. Seneor, A. Fert, *Nat. Phys.* **2012**, *8*, 557.
[13] Yu. S. Dedkov, M. Fonin, C. Laubschat, *Appl. Phys. Lett.* **2008**, *92*, 052506.
[14] S. Stepanow, P. S. Miedema, A. Mugarza, G. Ceballos, P. Moras, J. C. Cezar, C. Carbone, F. M. F. de Groot, P. Gambardella, *Phys. Rev. B* **2011**, *83*, 220401.
[15] P. Carra, B. T. Thole, M. Altarelli, X. Wang, *Phys. Rev. Lett.* **1993**, *70*, 694.
[16] M. Bernien, J. Miguel, C. Weis, Md. E. Ali, J. Kurde, B. Krumme, P. M. Panchmatia, B. Sanyal, M. Piantek, P. Srivastava, K. Baberschke, P. M. Oppeneer, O. Eriksson, W. Kuch, H. Wende, *Phys. Rev. Lett.* **2009**, *102*, 047202.
[17] Y. Li, K. Baberschke, *Phys. Rev. Lett.* **1992**, *68*, 1208.
[18] H. Wende, M. Bernien, J. Luo, C. Sorg, N. Ponpandian, J. Kurde, J. Miguel, M. Piantek, X. Xu, Ph. Eckhold, W. Kuch, K. Baberschke, P. M. Panchmatia, B. Sanyal, P. M. Oppeneer, O. Eriksson, *Nat. Mater.* **2007**, *6*, 516.
[19] Yu. S. Dedkov, M. Fonin, *New J. Phys.* **2010**, *12*, 125004.
[20] W. Zhao, S. M. Kozlov, O. Höfert, K. Gotterbarm, M. P. A. Lorenz, F. Vines, C. Papp, A. Görling, H.-P. Steinrück, *J. Phys. Chem. Lett.* **2011**, *2*, 759.
[21] U. Usachov, A. M. Dobrotvorskii, A. Varykhalov, O. Rader, W. Gudat, A. M. Shikin, V. K. Adamchuk, *Phys. Rev. B* **2008**, *78*, 085403.
[22] J. Lahiri, Y. Lin, P. Bozkurt, I. I. Oleynik, M. Batzill, *Nat. Nanotechnol.* **2010**, *5*, 326.
[23] B. Bäcker, G. Hörz, *Vacuum* **1995**, *46*, 1101.
[24] M. Fuentes-Cabrera, M. I. Baskes, A. V. Melechko, M. L. Simpson, *Phys. Rev. B* **2008**, *77*, 035405.

[25] S. Grimme, *J. Comp. Chem.* **2006**, *27*, 1787.
[26] B. Li, L. Chen, X. Pan, *Appl. Phys. Lett.* **2011**, *98*, 133111.
[27] J. Mao, H. Zhang, Y. Jiang, Y. Pan, M. Gao, W. Xiao, H.-J. Gao, *J. Am. Chem. Soc.* **2009**, *131*, 14136.
[28] A. Scheybal, T. Ramsvik, R. Bertschinger, M. Putero, F. Nolting, T. A. Jung, *Chem. Phys. Lett.* **2005**, *411*, 214.
[29] A. Lodi Rozzini, C. Krull, T. Balashov, J. J. Kavich, A. Mugarza, P. S. Miedema, P. K. Thakur, V. Sessi, S. Klyatskaya, M. Ruben, S. Stepanow, P. Gambardella, *Phys. Rev. Lett.* **2011**, *107*, 177205.
[30] J. B. Goodenough, *Magnetism and the Chemical Bond*, Wiley, New York **1963**.
[31] C. F. Hermanns, M. Bernien, A. Krüger, J. Miguel, W. Kuch, *J. Phys.: Condens. Matter* **2012**, *24*, 394008.
[32] M. Farle, A. Berghaus, Y. Li, K. Baberschke, *Phys. Rev. B* **1990**, *42*, 4873.
[33] P. M. Panchmatia, B. Sanyal, P. M. Oppeneer, *Chem. Phys.* **2008**, *343*, 47.
[34] Md. E. Ali, B. Sanyal, P. M. Oppeneer, *J. Phys. Chem. C* **2009**, *113*, 14381.
[35] P. E. Blöchl, *Phys. Rev. B* **1994**, *50*, 17953.
[36] G. Kresse, J. Furthmüller, *Phys. Rev. B* **1996**, *54*, 11169.
[37] J. P. Perdew, K. Burke, M. Ernzerhof, *Phys. Rev. Lett.* **1996**, *77*, 3865.